Atomic-Scale Investigation on the Facilitation and Inhibition of Guanine Tautomerization at Au(111) Surface

Huihui Kong,[†] Qiang Sun,[†] Likun Wang, Qinggang Tan, Chi Zhang, Kai Sheng, and Wei Xu*

College of Materials Science and Engineering, Key Laboratory for Advanced Civil Engineering Materials (Ministry of Education), Tongji University, Caoan Road 4800, Shanghai 201804, People's Republic of China. [†]These authors contributed equally to this work.

ABSTRACT Nucleobase tautomerization might induce mismatch of base pairing. Metals, involved in many important biophysical processes, have been theoretically proven to be capable of affecting tautomeric equilibria and stabilities of different nucleobase tautomers. However, direct real-space evidence on demonstrating different nucleobase tautomers and further revealing the effect of metals on their tautomerization at surfaces has not been reported to date. From the interplay of high-resolution STM imaging and DFT calculations, we show for the first time that tautomerization of guanine from G/9H to G/7H is facilitated on Au(111) by heating, whereas such tautomerization process is effectively inhibited by introducing Ni atoms due to its preferential coordination at the N7 site of G/9H. These findings may help to elucidate possible influence of metals on nucleobase tautomerization and provide from a molecular level some theoretical basis on metal-based drug design.

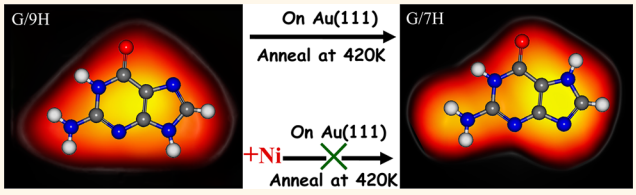

KEYWORDS: scanning tunneling microscopy · density functional theory · guanine tautomerization

Tautomerization, a ubiquitous phenomenon accompanied by transfer of a hydrogen atom or proton, has been found to extensively exist in N-heterocyclic compounds such as nucleobases.[1,2] In biological systems, the transformation of nucleobases from canonical forms to their noncanonical tautomeric forms could induce mismatch of base pairing and further disturb the genetic codes.[3] Due to the significance of nucleobase tautomerization, many experimental and theoretical efforts have been devoted to investigate the possible forms and stabilities of different tautomers by spectroscopic methods and DFT calculations.[2,4−7] Specifically, metals that are involved in many important biophysical processes have been found to be capable of affecting the tautomeric equilibria and further changing the orders of stabilities of different nucleobase tautomers.[8−10] Direct real-space evidence on demonstrating different nucleobase tautomers and further revealing the effect of metals on their tautomerization at surfaces, however, has not been reported to date. In particular, the local microscopic information, which is a key to understand fundamental issues, such as the structural aspects of different nucleobase tautomers, the binding sites of nucleobase tautomers with metals, the competition between different sites, needs to be urgently supplemented. Therefore, it is of importance to investigate the nucleobase tautomerization and explore the role of metals in this process in real space with the aim of getting a deeper understanding of the influence of metals on DNA base pairing and high-fidelity replication, which may also shed light on the potential applications in drug design.

Guanine (G), one of the biologically important purines existing in both DNA and RNA, is known to have many different tautomers.[11,12] Among these tautomers, the two most stable ones,[9,11] the canonical form (G/9H) and one of the noncanonical forms (G/7H), are illustrated in Figure 1. It is also well-known that G could form the so-called G-quadruplex structure (only by G canonical form (G/9H)) which has been treated as the potential anticancer drug target. In this article, we have investigated the facilitation and inhibition of G tautomerization on the Au(111) surface under ultrahigh vacuum (UHV) conditions. For this kind

* Address correspondence to xuwei@tongji.edu.cn.

Received for review December 2, 2013 and accepted January 29, 2014.

Published online January 29, 2014
10.1021/nn4061918

of study, scanning tunneling microscopy (STM) has proven to be the technique of choice since it allows a direct, real-space determination of topographies of different tautomers,[13,14] hydrogen-bonded structural motifs, and binding sites between molecules and metals[15,16] at the atomic scale. From the interplay of high-resolution STM imaging and density functional theory (DFT) calculations, we show for the first time that G molecules undergo a transition from G/9H to G/7H on Au(111) by heating, and a delicate control experiment of 7-methylguanine (7mG) on Au(111) corroborates the above tautomerization process. Surprisingly, when introducing Ni atoms, the tautomerization from G/9H to G/7H is effectively inhibited, and the formation of metallosupramolecular networks is facilitated in which G molecules are kept in the canonical form (G/9H). DFT calculations are performed to unravel this unexpected inhibition process, and the mechanism is proposed as follows: (1) the most stable binding site of G/9H coordinating with Ni is N7 which is exactly the site for proton transfer from N9 when tautomerization from G/9H to G/7H occurs; (2) once the N7 site is occupied by Ni, the tautomerization from G/9H to G/7H is automatically inhibited. These findings demonstrate that Ni atoms could effectively inhibit G tautomerization from G/9H to G/7H, in which the specific binding site is found to be the key. Such results may also help to elucidate the possible influence of metals on nucleobase tautomerization and provide from a molecular level some theoretical basis on metal-based drug design.

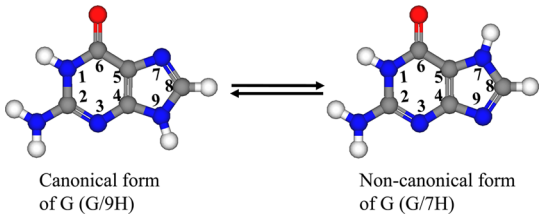

Figure 1. Two tautomeric forms of G: the canonical form G/9H (left) and one of the noncanonical forms G/7H (right). The tautomerization from G/9H to G/7H is caused by the proton transfer from N9 to N7. C, gray; N, blue; O, red; H, white.

RESULTS AND DISCUSSION

After deposition of G/9H molecules on Au(111) and subsequent anneal to 420 K, a well-ordered molecular network nanostructure is observed as shown in Figure 2a. The high-resolution close-up STM image (Figure 2b) reveals that the structure is formed by laterally connected zigzag ribbons separated by the dashed wavy lines. We could also distinguish the submolecularly resolved topography of individual molecules, and moreover, the molecular chiralities as indicated by R and L. Hence, we identify that each ribbon is formed by alternating R and L chiral forms, and the adjacent ribbons are antiparallel with respect to each other. Such self-assembled G nanostructure has been previously reported in the literature.[17,18] However, on the basis of detailed analyses (Figures S1−S5 in Supporting Information), we find that the previously proposed models based on G/9H form seem far-fetched to rationally explain the experimentally observed nanostructure.

It should be noted that the network structure shown in Figure 2 is only observed after anneal, as also reported in the literature.[17,18] Moreover, we learn from the literature[6] that thermal treatment could induce the nucleobase tautomerization. Hence, we tentatively speculate that after annealing the sample at 420 K G/9H molecules may have undergone the transition to one of its most stable tautomeric forms (G/7H) (cf. Figure 1). On the basis of this hypothesis, we then build up the models based on G/7H molecules. After relaxation, we obtain a quite stable structure with the binding energy of 1.4 eV/molecule (higher than the G-quartet network by ~0.3 eV/molecule), and furthermore, when superimposing this model on top of the close-up STM image, an excellent agreement is achieved, as demonstrated in Figure 2c. Also, comparison of the

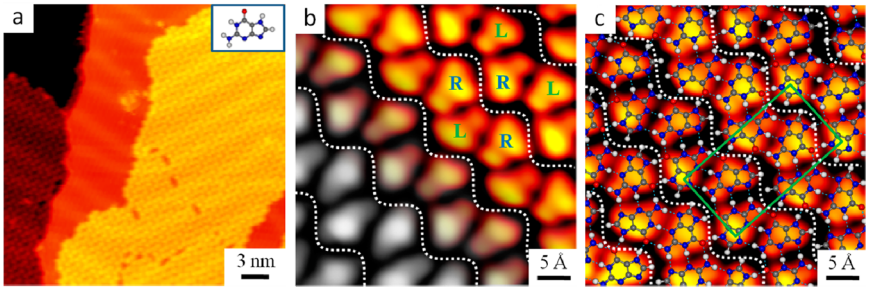

Figure 2. STM images, DFT-based optimized structural model, and simulated STM image of self-assembled molecular network formed by G/7H on Au(111). (a) STM image shows the formation of molecular network by G/7H. The inset shows the chemical structure of G/7H. (b) High-resolution close-up STM image allows us to distinguish the submolecularly resolved topography of individual molecule and molecular chiralities (as indicated in the image by R and L notation). The dashed wavy lines separate the adjacent antiparallel ribbons. The simulated STM image (the gray part) is partially superimposed on the STM image. (c) DFT-optimized structural model is superimposed on the close-up STM image where a good agreement is achieved. The green rectangle represents the unit cell of the network structure (scanning conditions: I_t = 0.88 nA, V_t = −1.25 V; STM image simulation at the bias voltage of −1.25 V).

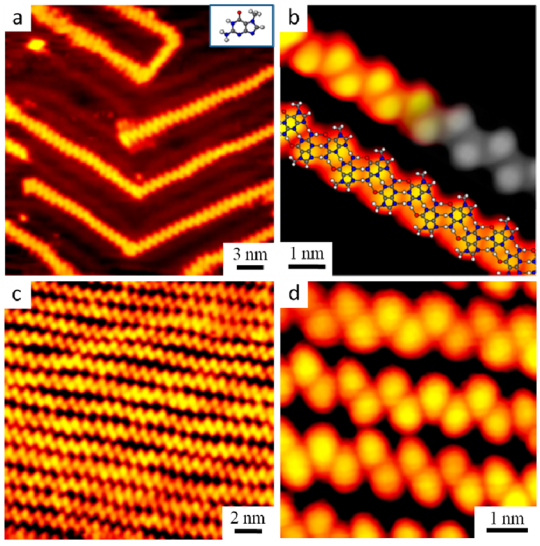

Figure 3. STM images, DFT-based optimized structural models, and simulated STM image of self-assembled molecular ribbon structures formed by 7mG on Au(111). (a) STM image shows the formation of molecular ribbons growing along the herringbone reconstruction of the Au(111) surface after deposition of 7mG onto the surface at RT. The inset shows the chemical structure of 7mG. (b) DFT-optimized structural model and simulated STM image (the gray part) are superimposed on the high-resolution close-up STM images, respectively. (c) STM image shows the densely packed molecular ribbons at high coverage after anneal at 420 K. (d) High-resolution close-up STM image of densely packed ribbons showing that the ribbon structure is stable after anneal at 420 K (scanning conditions: I_t = 0.83 nA, V_t = −1.25 V; STM image simulation at the bias voltage of −1.25 V).

experimental STM image with the simulated one (the gray part) depicted in Figure 2b illustrates that both the single-molecule topography and the structural motif correspond quite well. From the model (Figure 2c), we could identify that along the ribbons each G/7H molecule binds to the other two *via* a rather stable triple hydrogen bond (two N−H···N and one N−H···O), and between the ribbons, each G/7H molecule laterally binds to another by a double hydrogen bond (two N−H···O).

To further verify our speculation of G tautomerization and the proposed model, we conduct a delicate control experiment by choosing an analogue of the G/7H molecule, that is, 7-methylguanine (shortened as 7mG, the chemical structure is shown in the inset of Figure 3a), and compare the self-assembled nanostructure of 7mG with the one shown in Figure 2. Compared with the G/7H molecule, the H atom at N7 site is replaced by a methyl group in the 7mG molecule, and the other potential hydrogen-bonding donor and acceptor groups are exactly the same for these two molecules. Since the N7−H donor group of the G/7H molecule is not involved in the formation of a hydrogen-bonded ribbon structure (cf. Figure 2c) and is only for lateral connection between the ribbons, we hence speculate that the 7mG molecules should also form the similar hydrogen-bonded ribbon structure to the ones (separated by the dashed wavy lines) shown in Figure 2. After deposition of 7mG molecules on Au(111), we find that at low coverage 7mG molecules self-assemble into separated ribbons growing along the herringbone reconstruction of Au(111), as shown in Figure 3a. Figure 3b shows the high-resolution STM images of single ribbons overlaid by the DFT-optimized model and the simulated STM image (the gray part) where excellent agreements are achieved. We can recognize that this ribbon structure of 7mG has exactly the same hydrogen-bonded motif as the one shown in Figure 2. Furthermore, after annealing the high-coverage sample at 420 K, we find that the ribbon structure is still stable and the ribbons are separated because the potential hydrogen bonds between the ribbons are screened by methyl groups (cf. Figure 3c,d). From the above analyses, we then draw the conclusion that the surface nanostructure shown in Figure 2 is undoubtedly formed by G/7H molecules, and that is G tautomerization from G/9H to G/7H facilitated by thermal treatment unambiguously occurs on Au(111).

Furthermore, to explore the role of metals in G tautomerization, we choose a transition metal Ni to investigate the fundamental interactions between G and Ni. Sequential co-deposition of G/9H molecules and Ni atoms followed by anneal at 420 K leads to the formation of a kind of metallosupramolecular network structure with each island being homochiral, as shown in Figure 4a. This metallosupramolecular network structure is found to coexist with the nanostructure formed by G/7H (cf. Figure S6 in Supporting Information) if lower doses of Ni are deposited, and the ratios of these two intrinsically different nanostructures are sensitively dependent on the doses of Ni atoms. Figure 4b,c depicts high-resolution close-up STM images of enantiomerically pure R and L chiral structures, respectively, where the DFT-optimized structural models (with the binding energy of 2.5 eV/molecule) are superimposed and good agreements are achieved. The simulated STM image (the gray part) is also partially overlaid on top of the experimental one, where a good agreement is achieved as shown in Figure 4d, which further confirms the proposed model. From the model, we can identify that all the molecules are in the G canonical form G/9H and each G/9H molecule coordinates with the Ni atom at the N7 site. Interestingly enough, this N7 site happens to be the site for proton transfer from N9 when tautomerization from G/9H to G/7H occurs. Hence, we can draw the conclusion here, when the G/9H molecule coordinates with Ni atom at N7, this site is automatically screened for proton transfer, thus tautomerization from G/9H to G/7H is effectively inhibited.

To unravel this unexpected inhibition process of G tautomerization and the formation mechanism of metallosupramolecular network structure, detailed

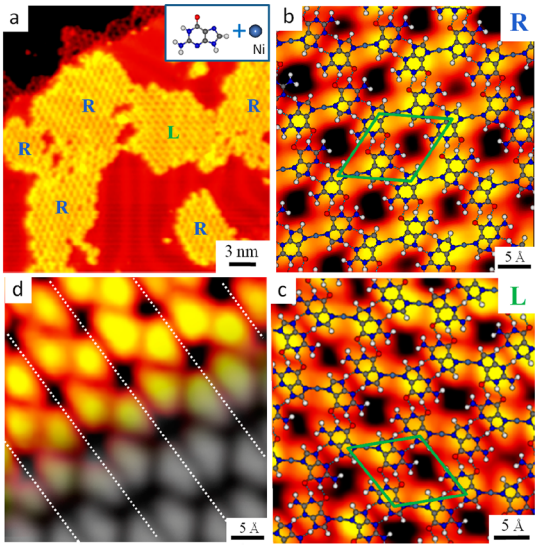

Figure 4. STM images, DFT-based optimized structural models, and simulated STM image of G/9H and Ni-coordinated metallosupramolecular network on Au(111). (a) STM image shows the self-assembled nanostructures with each island being homochiral (as indicated by R and L) formed by G/9H and Ni after annealing at 420 K. The inset shows the chemical structure of G/9H and Ni. (b,c) DFT-optimized structural models of R and L chiral metallosupramolecular network structures that are superimposed on the corresponding high-resolution close-up STM images where good agreements are achieved. The green parallelogram represents the unit cell of the nanostructure. (d) Simulated STM image (the gray part) is partially superimposed on the STM image; the dashed lines separate the adjacent zigzag chains (scanning conditions: I_t = 0.56 nA, V_t = −1.25 V; STM image simulation at the bias voltage of −1.25 V).

DFT analyses are performed. First, we start out the calculations by considering the Ni atom interacting with all the possible binding sites of G/9H molecule on Au(111). Figure 5a−c demonstrates the optimized models of one Ni atom coordinating with N7, O6, and N3 sites, respectively. From the calculations, we find that the N7 site is the most stable binding site for Ni (more stable than binding with O6 and N3 by 0.26 and 0.40 eV, respectively), which is the prerequisite for this inhibition process of G tautomerization. Second, further calculations are performed by placing two homochiral and heterochiral G/9H molecules interacting with one Ni atom on Au(111), as shown in Figure 5d,e, respectively. In this calculation, we have only considered N7 as the binding sites for both molecules, and

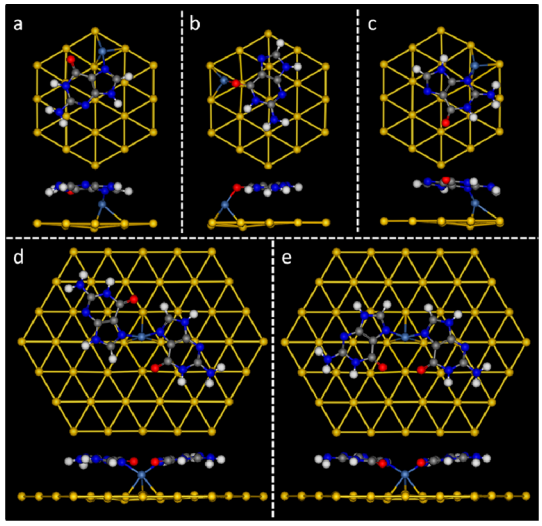

Figure 5. DFT-optimized models of Ni atom interacting with single and two G/9H molecules on Au(111). (a−c) Top and side views of DFT-optimized models of Ni atom interacting with single G/9H molecule at N7, O6, and N3 sites, respectively. (d,e) Top and side views of DFT-optimized models of Ni atom interacting with two homochiral and two heterochiral G/9H molecules at the N7 site, respectively.

after relaxation, we find that the structure formed by two homochiral molecules coordinating with Ni (cf. Figure 5d) is energetically more favorable than the heterochiral ones (cf. Figure 5e) by 0.20 eV. The structural motif shown in Figure 5d is the fundamental building block of the metallosupramolecular networks shown in Figure 4b,c. Hence, G tautomerization from G/9H to G/7H is inhibited by the preferential coordination of Ni at N7 site of G molecule.

CONCLUSION

In conclusion, from the interplay of submolecularly resolved STM imaging and DFT calculations, we have demonstrated that G tautomerization from canonical form G/9H to noncanonical form G/7H could be facilitated by heating on Au(111), and when Ni atoms are introduced, this tautomerization process could be, however, effectively inhibited. Additional experiments on exploring other metals interacting with nucleobases are in progress to get a deeper understanding of the roles metal plays in biologically relevant processes. Such model systems may also provide theoretical guidance for potential design of novel metal-based drugs.

METHODS AND MATERIALS

All STM experiments were performed in a UHV chamber (base pressure 1 × 10^{-10} mbar) equipped with the variable-temperature, fast-scanning "Aarhus-type" STM,[19,20] a molecular evaporator and an e-beam evaporator, and other standard instrumentation for sample preparation. The Au(111) substrate was prepared by several cycles of 1.5 keV Ar^+ sputtering followed by annealing to 770 K for 15 min, resulting in clean and flat terraces separated by monatomic steps. The G molecules were loaded into a glass crucible in the molecular evaporator. After a thorough degassing, G molecules and 7mG molecules were deposited onto the clean substrate by thermal sublimation at 420 and 390 K, respectively; the Ni atoms were sequentially deposited onto the G-covered surfaces at RT. After preparation, the samples were imaged by STM over a temperature range of 100−150 K. The calculations were

performed in the framework of DFT by using the Vienna ab initio simulation package (VASP).[21,22] The projector-augmented wave method was used to describe the interaction between ions and electrons; the Perdew–Burke–Ernzerhof generalized gradient approximation exchange-correlation functional was employed,[23] and van der Waals interactions were included using the dispersion-corrected DFT-D2 method of Grimme[24] for the calculations when including the gold surface. The atomic structures were relaxed using the conjugate gradient algorithm scheme as implemented in the VASP code until the forces on all unconstrained atoms were $\leq$0.03 eV/Å. The simulated STM images were based on the Tersoff–Hamann method.[25]

Conflict of Interest: The authors declare no competing financial interest.

Acknowledgment. The authors acknowledge the financial support from the National Natural Science Foundation of China (21103128), the Shanghai "Shu Guang" project supported by Shanghai Municipal Education Commission and Shanghai Education Development Foundation (11SG25), the Fundamental Research Funds for the Central Universities, the Research Fund for the Doctoral Program of Higher Education of China (20120072110045).

Supporting Information Available: Different models based on G/9H; STM image and the model of G-quartet structure; larger-scale STM images of Figures 2 and 4. This material is available free of charge *via* the Internet at http://pubs.acs.org.

REFERENCES AND NOTES

1. Topal, M. D.; Fresco, J. R. Complementary Base-Pairing and the Origin of Substitution Mutations. *Nature* **1976**, *263*, 285–289.
2. Choi, M. Y.; Miller, R. E. Four Tautomers of Isolated Guanine from Infrared Laser Spectroscopy in Helium Nanodroplets. *J. Am. Chem. Soc.* **2006**, *128*, 7320–7328.
3. Lowdin, P. O. Proton Tunneling in DNA and Its Biological Implications. *Rev. Mod. Phys.* **1963**, *35*, 724–732.
4. Douhal, A.; Kim, S. K.; Zewail, A. H. Femtosecond Molecular Dynamics of Tautomerization in Model Base Pairs. *Nature* **1995**, *378*, 260–263.
5. Nir, E.; Janzen, C.; Imhof, P.; Kleinermanns, K.; de Vries, M. S. Guanine Tautomerism Revealed by UV–UV and IR–UV Hole Burning Spectroscopy. *J. Chem. Phys.* **2001**, *115*, 4604–4611.
6. Padermshoke, A.; Katsumoto, Y.; Masaki, R.; Aida, M. Thermally Induced Double Proton Transfer in GG and Wobble GT Base Pairs: A Possible Origin of the Mutagenic Guanine. *Chem. Phys. Lett.* **2008**, *457*, 232–236.
7. Serrano-Andres, L.; Merchan, M.; Borin, A. C. A Three-State Model for the Photophysics of Guanine. *J. Am. Chem. Soc.* **2008**, *130*, 2473–2484.
8. Kabelac, M.; Hobza, P. Na^+, Mg^{2+}, And Zn^{2+} Binding to All Tautomers of Adenine, Cytosine, and Thymine and the Eight Most Stable Keto/Enol Tautomers of Guanine: A Correlated *Ab Initio* Quantum Chemical Study. *J. Phys. Chem. B* **2006**, *110*, 14515–14523.
9. Russo, N.; Toscano, M.; Grand, A. Bond Energies and Attachments Sites of Sodium and Potassium Cations to DNA and RNA Nucleic Acid Bases in the Gas Phase. *J. Am. Chem. Soc.* **2001**, *123*, 10272–10279.
10. Russo, N.; Toscano, M.; Grand, A. Gas-Phase Absolute Ca^{2+} and Mg^{2+} Affinity for Nucleic Acid Bases. A Theoretical Determination. *J. Phys. Chem. A* **2003**, *107*, 11533–11538.
11. Dolgounitcheva, O.; Zakrzewski, V. G.; Ortiz, J. V. Electron Propagator Theory of Guanine and Its Cations: Tautomerism and Photoelectron Spectra. *J. Am. Chem. Soc.* **2000**, *122*, 12304–12309.
12. Chung, G.; Oh, H.; Lee, D. Tautomerism and Isomerism of Guanine–Cytosine DNA Base Pair: *Ab Initio* and Density Functional Theory Approaches. *J. Mol. Struct. (THEOCHEM)* **2005**, *730*, 241–249.
13. Liljeroth, P.; Repp, J.; Meyer, G. Current-Induced Hydrogen Tautomerization and Conductance Switching of Naphthalocyanine Molecules. *Science* **2007**, *317*, 1203–1206.
14. Auwärter, W.; Seufert, K.; Bischoff, F.; Ecija, D.; Vijayaraghavan, S.; Joshi, S.; Klappenberger, F.; Samudrala, N.; Barth, J. V. A Surface-Anchored Molecular Four-Level Conductance Switch Based on Single Proton Transfer. *Nat. Nanotechnol.* **2012**, *7*, 41–46.
15. Marschall, M.; Reichert, J.; Weber-Bargioni, A.; Seufert, K.; Auwärter, W.; Klyatskaya, S.; Zoppellaro, G.; Ruben, M.; Barth, J. V. Random Two-Dimensional String Networks Based on Divergent Coordination Assembly. *Nat. Chem.* **2010**, *2*, 131–137.
16. Langner, A.; Tait, S. L.; Lin, N.; Chandrasekar, R.; Meded, V.; Fink, K.; Ruben, M.; Kern, K. Selective Coordination Bonding in Metallo-supramolecular Systems on Surfaces. *Angew. Chem., Int. Ed.* **2012**, *51*, 4327–4331.
17. Heckl, W. M.; Smith, D. P.; Binnig, G.; Klagges, H.; Hänsch, T. W.; Maddocks, J. Two-Dimensional Ordering of the DNA Base Guanine Observed by Scanning Tunneling Microscopy. *Proc. Natl. Acad. Sci. U.S.A.* **1991**, *88*, 8003–8005.
18. Otero, R.; Schöck, M.; Molina, L. M.; Lægsgaard, E.; Stensgaard, I.; Hammer, B.; Besenbacher, F. Guanine Quartet Networks Stabilized by Cooperative Hydrogen Bonds. *Angew. Chem., Int. Ed.* **2005**, *44*, 2270–2275.
19. Besenbacher, F. Scanning Tunnelling Microscopy Studies of Metal Surfaces. *Rep. Prog. Phys.* **1996**, *59*, 1737–1802.
20. Lægsgaard, E.; Osterlund, L.; Thostrup, P.; Rasmussen, P. B.; Stensgaard, I.; Besenbacher, F. A High-Pressure Scanning Tunneling Microscope. *Rev. Sci. Instrum.* **2001**, *72*, 3537–3542.
21. Kresse, G.; Hafner, J. *Ab Initio* Molecular Dynamics for Open-Shell Transition Metals. *Phys. Rev. B* **1993**, *48*, 13115–13118.
22. Kresse, G.; Furthmuller, J. Efficient Iterative Schemes for *Ab Initio* Total-Energy Calculations Using a Plane-Wave Basis Set. *Phys. Rev. B* **1996**, *54*, 11169–11186.
23. Perdew, J. P.; Burke, K.; Ernzerhof, M. Generalized Gradient Approximation Made Simple. *Phys. Rev. Lett.* **1996**, *77*, 3865–3868.
24. Grimme, S. Semiempirical GGA-Type Density Functional Constructed with a Long-Range Dispersion Correction. *J. Comput. Chem.* **2006**, *27*, 1787–1799.
25. Tersoff, J.; Hamann, D. R. Theory of the Scanning Tunneling Microscope. *Phys. Rev. B* **1985**, *31*, 805–813.